

*Supporting Information (SI)*

# FUSED DEPOSITION MODELING 3D PRINTING FOR (BIO)ANALYTICAL DEVICE FABRICATION: PROCEDURES, MATERIALS AND APPLICATIONS

---

G. IJ. Salentijn<sup>ab</sup>, P. E. Oomen<sup>a</sup>, M. Grajewski<sup>a</sup>, E. Verpoorte<sup>a†</sup>

<sup>a</sup> Pharmaceutical Analysis, Groningen Research Institute of Pharmacy, University of Groningen, THE NETHERLANDS

<sup>b</sup> TI-COAST, Science Park 904, 1098 XH Amsterdam, THE NETHERLANDS

† Corresponding author

***Table of contents:***

**EXPERIMENTAL**

CHARACTERIZATION OF A BENCHTOP FDM PRINTER

- Page S-3: *Protocol S1*: Characterization of resolution, surface roughness, and overhang  
*Figure S1*: SolidWorks design to assess resolution, surface roughness and overhang
- Page S-4: *Protocol S2*: Prevention of leakage  
*Figure S2*: SolidWorks design and slice settings for leakage tests
- Page S-5: *Protocol S3*: Transparency  
*Figure S3*: SolidWorks design for a device compatible with microscopy
- Page S-6: *Table S1*: Slice and print settings for various test parts

POLYMERS FOR FDM PRINTING

- Page S-7: *Table S2*: Print settings for 12 FDM filament materials
- Page S-8: *Protocol S4*: Autofluorescence
- Page S-9: *Protocol S5*: Solvent compatibility  
*Table S3*: Classification of solvent compatibility
- Page S-10: *Protocol S6*: Biocompatibility tests

APPLICATIONS OF FDM PRINTING

- Page S-14: *Protocol S7*: PDMS replication and device fabrication
- Page S-15: *Protocol S8*: Wax patterning for paper microfluidics with 3D-printed tools  
*Figure S4*: SolidWorks drawings for the tool parts used in the wax-dipping approach

**RESULTS**

POLYMERS FOR FDM PRINTING

- Page S-16: *Figure S5*: Autofluorescence of FDM materials (photographs)
- Page S-17: *Figure S6*: Autofluorescence of FDM materials (numerical)
- Page S-18: *Figure S7*: Solvent compatibility study of FDM materials (numerical)
- Page S-18: *Figure S8*: Photographs of 3D-printed models after exposure to different solvents
- Page S-20: *Figure S9*: Biocompatibility of FDM materials
- Page S-21: *Figure S10*: Photographs of HUVEC in contact with FDM materials
- Page S-22: *Figure S11*: Boxplot HUVEC biocompatibility data (MTT assay)
- Page S-23: *Figure S12*: Boxplot PCLS biocompatibility data (LDH leakage assay)
- Page S-24: *Figure S13*: Boxplot PCLS biocompatibility data (ATP assay)
- Page S-25: *References*

**Protocol S1:** Characterization of resolution, surface roughness, and overhang.

Embedded channels (rectangular, circular and diamond-shaped) were printed in red PLA (EasyFil, Formfutura, Nijmegen, The Netherlands) with dimensions ranging from 0.1 to 5.0 mm with an aspect ratio of 1 (Figure S1). The structures were illuminated from both sides to visualize the surface and the channel under a microscope (Leica S8APO, Leica Microsystems, Wetzlar, Germany). Slice and print settings are listed in Table S1.

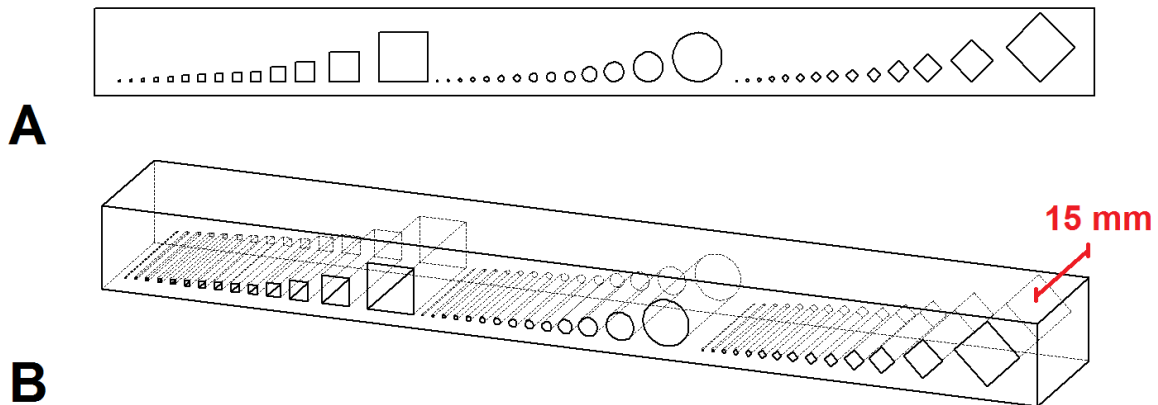


**Figure S1:** SolidWorks model to characterize printing resolution and assess the impact of overhanging structures such as channel ceilings in different designs. The structure shown in the SolidWorks drawings contains embedded channels having rectangular, circular, or diamond-shaped cross-sections of varying sizes. (A) Front view of the structure with embedded channels. (B) 3D view of the same structure as in (A). Three different cross-sectional channel shapes were tested (square, circular and diamond-shaped). The diameter (circular) or diagonal width (square, diamond-shaped) was varied (from left to right, in mm: 0.1, 0.2, 0.3, 0.4, 0.5, 0.6, 0.7, 0.8, 0.9, 1.0, 1.5, 2.0, 3.0, 5.0), while the aspect ratio was kept constant at 1 (channel height = channel width).

**Protocol S2: Prevention of leakage**

An embedded channel (l = 15 mm, w = 0.8 mm, h = 0.8 mm) with an inlet and outlet reservoir (ID = 4 mm) was printed in Transparent PLA (Figure S2A). The part was printed with different *infill solidities* and *shell numbers* (Table S1, Figure S2B). After the parts were printed, 50  $\mu$ L of a methanol/water solution (1:1 (v/v)) of blue food dye (Jo-La, E131, Bharmco Foods, Braambrugge, The Netherlands) was introduced to the inlet reservoirs to fill the channels, and photographs were taken.

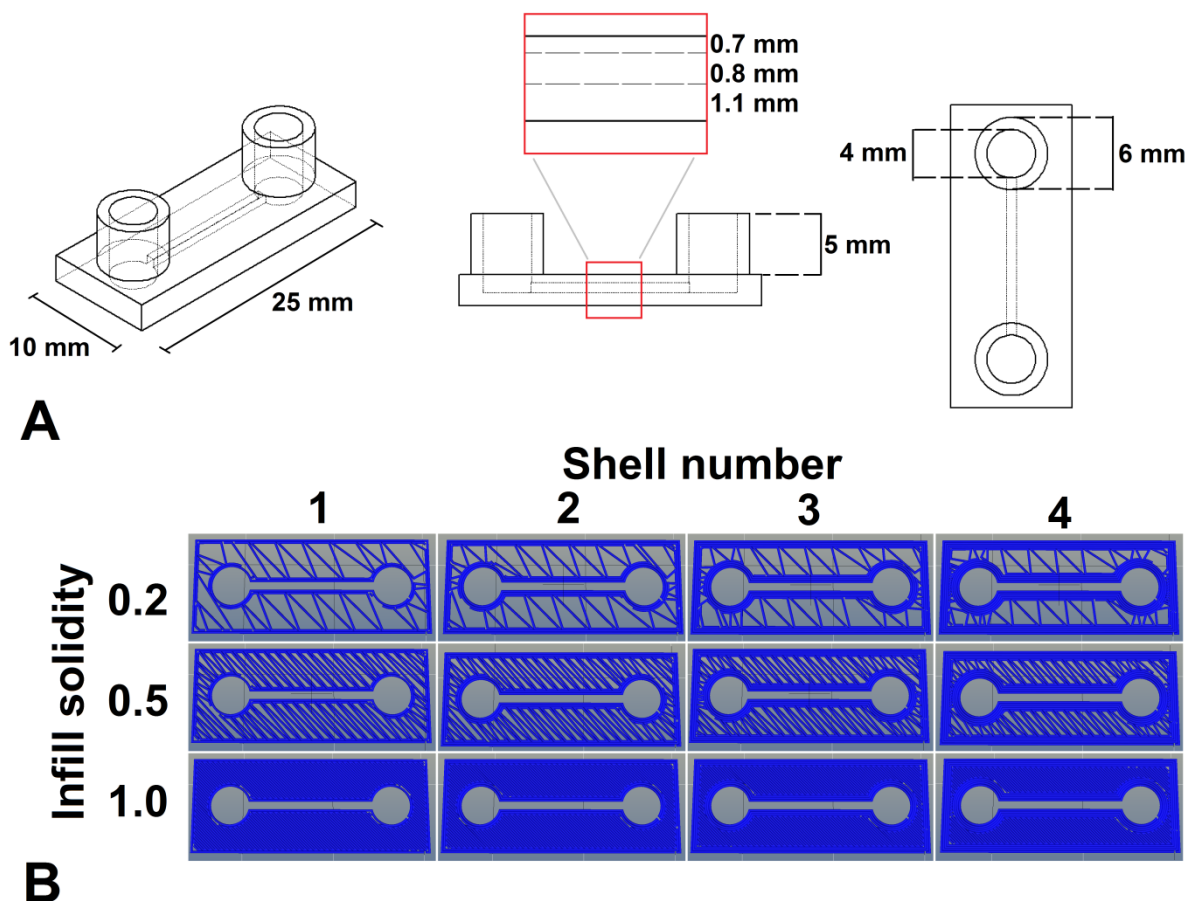


**Figure S2:** (A) SolidWorks design for a device to test prevention of leakage in 3D-printed channels. The embedded channel has a length of 15 mm, width of 0.8 mm and depth of 0.8 mm. The thickness of the PLA channel ceiling is 0.7 mm, whereas the channel base is 1.1 mm thick. (B) Different infill solidities and shell numbers were set in the slicing software to assess their impact on the prevention of leakage.

### Protocol S3: Transparency

A device was designed with an internal cavity that acted as a frame for a glass microscope slide (Table S1, Figure S3) and printed in Transparent PLA. Once the device had been printed up to the point where the cavity walls were completed, the print was paused, and the glass slide was inserted into the cavity. The print was then continued, and sealed channels were printed on top of the glass slide (*i.e.* the glass slide served as the bottom of the channel). Once finished, the channels were filled with aqueous blue dye solution and imaged from the top and bottom through the PLA and glass layers, respectively. The transparency of the PLA device could be characterized qualitatively in this way.

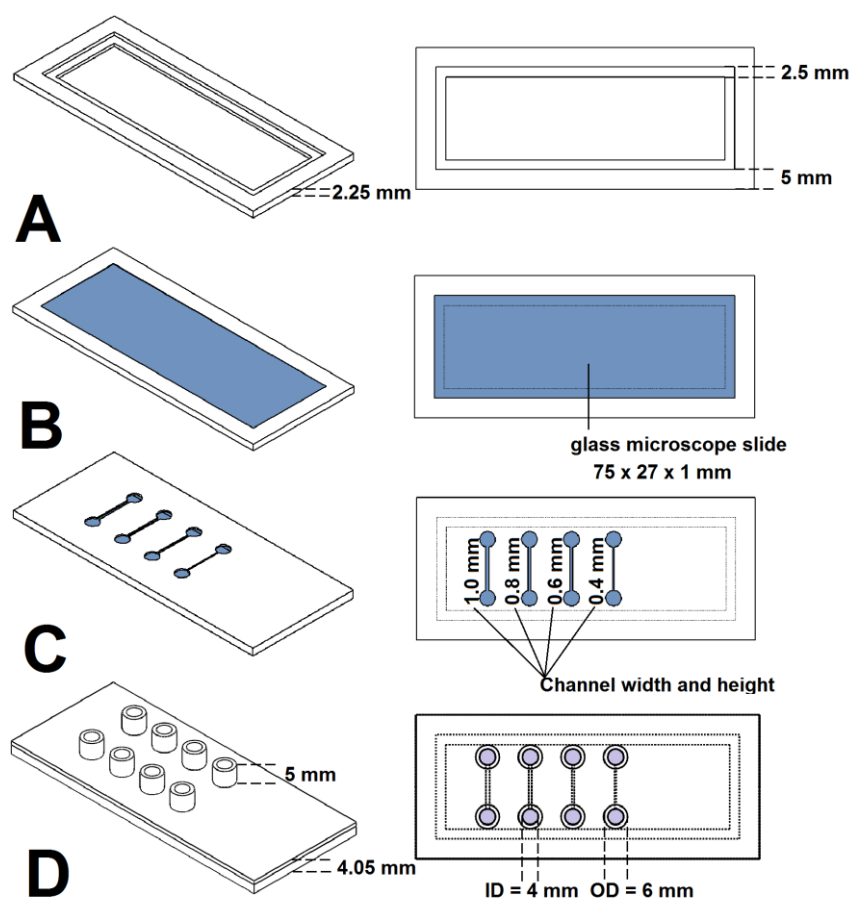


**Figure S3:** Hybrid PLA/glass device to test transparency. A hollow frame was designed in SolidWorks, with an internal cavity the size of a microscope glass slide (27 mm by 75 mm by 1 mm). The device was printed in Transparent PLA. (A) The device was printed up to the point where the cavity walls were completed. (B) The print was then paused and the glass slide (blue) was inserted into the cavity, to form the bottom exterior surface of the device. (C) The print was then continued and PLA channels were printed onto the glass slide, which served as the bottom of the channels. (D) The rectangular channels were sealed by printing transparent PLA over them, and solvent reservoirs were printed on the inlets and outlets of the channels.

**Table S1:** Slice and print information for various 3D-printed test structures and devices

<b>Process</b>	<b>Parameter</b>	<b>Structure for resolution test and PDMS replication molding</b>	<b>Device for leakage prevention test</b>	<b>Device for transparency test</b>
<b>Slicing</b>	<i>Resolution</i>	0.13 mm (z) 0.26 mm (xy)	0.13 mm (z) 0.26 mm (xy)	0.13 mm (z) 0.26 mm (xy)
	<i>Infill solidity<sup>a</sup></i>	1	0.2, 0.5, 1.0	1
	<i>Infill pattern</i>	n/a	Line	n/a
	<i>Shell nr.<sup>b</sup></i>	1	1, 2, 3, 4	2
<b>Printing</b>	<i>Printing speed (perimeter / infill)</i>	25 mm/s; 40 mm/s	25 mm/s; 40 mm/s	25 mm/s; 40 mm/s
	<i>Extruder temp.</i>	200 °C	200 °C	200 °C
	<i>Print bed temp.</i>	60 °C	60 °C	60 °C
	<i>Filament type</i>	PLA EasyFil, red	Transparent PLA	Transparent PLA
<b>Miscellaneous</b>		n/a	n/a	Insert glass slide during the print

<sup>a</sup> Ratio between filament and air in the interior of the part. A low Infill solidity value (e.g. 0.2) leads to a relatively open infill, whereas a high value (e.g. 1) leads to a solid part. See also Fig. S2.

<sup>b</sup> Number of adjacent threads of filament that outline all structures.

**Table S2:** List of tested FDM materials and printing parameters.

Material	Chemical composition	Filament Supplier	Extruder temp. (°C)	Bed temp. (°C)	Rel. print speed <sup>a</sup> (mm/s)	Extruder fan	Brim <sup>b</sup>
<b>PLA Gold (EasyFil)</b>	poly (lactic acid)	FormFutura	200	60	100%	On	No
<b>Transparent PLA (Premium)</b>	poly (lactic acid)	FormFutura	200	60	100%	On	No
<b>PLA Soft</b>	poly (lactic acid)	Orbi-Tech	210	60	50%	On	No
<b>PLA 45</b>	poly (lactic acid)	Orbi-Tech	170	55	100%	On	No
<b>ABS Orange</b>	acrylonitrile butadiene styrene	Kunststofshop	225	80	100%	Off	Yes
<b>PC</b>	polycarbonate	Orbi-Tech	250	80	100%	Off	Yes
<b>PS</b>	polystyrene	FormFutura	215	80	100%	On	Yes
<b>PVA</b>	poly (vinyl alcohol)	Orbi-Tech	185	55	100%	On	No
<b>PET</b>	poly (ethylene terephthalate)	FormFutura	210	65	100%	On	No
<b>T-Glase</b>	poly (ethylene terephthalate)	Taulman 3D	210	65	100%	On	No
<b>Arnitel Eco</b>	thermoplastic co-polyester	Formfutura (DSM)	210	60	60%	On	No
<b>Bendlay</b>	acrylnitrile butadiene styrene	Orbi-Tech	210	65	100%	On	No

<sup>a</sup> Print speed can be predefined in the slicing software. During the print, this speed is regarded as the ‘100%’ value. Print speeds can be adjusted to values between 25% and 300% of the predefined value during the print. In general, for the structures that were printed to test material properties, a basic print speed of 70 mm/s for the infill and 40 mm/s for the perimeter shells was used.

<sup>b</sup> A number of additional shells is printed around the first layer, in order to increase the surface of this layer and thus improve the attachment to the plate. Furthermore, the use of a brim can reduce warping effects.

***Protocol S4: Autofluorescence***

The autofluorescence of each material was evaluated under an inverted fluorescence microscope (DM-IL, Leica Microsystems, Wetzlar, Germany) equipped with a Leica DFC300 FX camera (Leica Microsystems, Wetzlar, Germany), for three different wavelength ranges. Y3 ET (ex/em 530-557/575-647 nm), GFP ET (ex/em 450-488/505-545 nm) and CFP ET (ex/em 430-445/460-500 nm) filter cubes were used. Photographs were acquired with an acquisition time of 50 milliseconds. The average color intensity of the photographs was measured using ImageJ<sup>1</sup>. The autofluorescence of the materials was classified based on the intensity data.



**Protocol S5: FDM materials: Solvent compatibility test**

Test structures were printed with all twelve materials to assess their compatibility with water, methanol, acetonitrile, isopropanol and acetone. The test structure was a 2D generic human figure, selected because it combines relatively thick (torso, approximately 5 mm) and thin (limbs, approximately 1 mm) features in one structure (approximately 14 mm tall). Fifteen test structures were printed in each of the 12 FDM materials of interest, 3 for each solvent tested. Each preweighed test structure was put into an individual, preweighed, labeled Eppendorf tube (*exposure tube*). One mL of the solvent to be tested was added to each of three exposure tubes to initiate exposure. Three exposure times were tested, namely 1 hour, 24 hours (1 day) and 168 hours (7 days). During exposure, the tubes were placed on a PS-3D shaker at approximately 40 rpm (Grant Instruments, Cambridgeshire, UK). After the set exposure time had passed, 0.5 mL of the solvent was removed from the tube and placed into a labelled, preweighed Eppendorf tube (*evaporation tube*). The evaporation tube was not sealed, so as to allow the solvent to evaporate in a fume hood. The polymer figure was photographed immediately after the end of exposure. The remaining solvent in the exposure tube was then removed, and the model was allowed to dry in this tube for at least a day. Afterwards, the weight of the material in the evaporation tube was determined as an indication of the amount of material that had dissolved into the solvent. The weight of the dried figure after exposure was also determined. Polymer solvent compatibility was classified based on the following rules:

**Table S3: Classification of solvent compatibility**

<b>Rule (in order of priority)</b>	<b>Classification</b>
Dissolved material > 10% of initial mass	--
> 10 % deviation from initial mass in remaining material	--
Loss of structural integrity	--
Dissolved material > 5 % of initial mass	-
> 5 % deviation from initial mass in remaining material	-
Obvious swelling or change in color	-
Dissolved material > 2.5 % of initial mass	+/-
> 2.5 % deviation from initial mass in remaining material	+/-
Dissolved material < 2.5 % of initial mass	+
< 2.5 % deviation from initial mass in remaining material	+

### **Protocol S6: Biocompatibility tests**

**Cell model:** Human umbilical vein endothelial cells (HUVEC) were selected because of their high sensitivity to changes in culture conditions and broad application in studies of drug mechanisms, wound healing, immune response, oxidative stress, and arteriosclerosis<sup>2</sup>. They constitute a more sensitive and representative model for biocompatibility studies than immortalized cell lines. HUVEC (Lonza, CC-2519, pooled donors, Benelux B.V., Breda, The Netherlands) were cultured to confluency in T25 flasks for 2 to 4 passages before being seeded in 12-well plates. HUVEC were harvested from T25 bottles by trypsinization (0.05% trypsin solution in sterile PBS; 20  $\mu\text{L}/\text{cm}^2$  of trypsin solution), counted and resuspended in fresh endothelial cell (EC) medium at a concentration of 4500 cells/ $\mu\text{L}$ . Afterwards they were kept on ice until further use. The Eppendorf tube containing the cells was gently shaken to resuspend the cells just before seeding 5  $\mu\text{L}$  in 12-well plates, which had been coated with a 1% solution of gelatin (porcine skin, Sigma Aldrich, Steinheim, Germany) according to the supplier's protocol.

**Cell cultivation conditions:** Endothelial cell medium (EC medium) consisted of RPMI 1640 (Lonza Benelux B.V., Breda, The Netherlands); endothelial cell growth factor (50  $\mu\text{g}/\text{mL}$  isolated from bovine brain); L-glutamine (2 mM; Gibco-BRL, Paisley, Scotland); heparin (5 U; Leo Pharm. Prod., Weesp, The Netherlands); K-penicillin G (100 IE/mL; Astellas Pharma Europe B.V., Leiderdorp, The Netherlands); streptomycin (100  $\mu\text{g}/\text{mL}$ ; Fisiopharm, Italy); and fetal calf serum (20% v/v; Hyclone, Perbio Science, Etten-Leur, The Netherlands). The medium did not contain the pH indicator, phenol red. For the exposure experiments, HUVEC were incubated (Esco Cell Culture CO<sub>2</sub> Incubator) in 12-well plates at 37°C, with 95% air and 5% CO<sub>2</sub>. Polymer exposure/biocompatibility tests were started when HUVEC cultures had achieved 60-80% confluency, which was generally the case after an overnight cultivation. Fresh medium was added at the start of the experiment and was not refreshed for the duration of the experiment (18h). After addition of medium, 3D-printed rings (ID 17 mm; OD 21 mm, thickness 1 mm) were placed in the wells. In addition, HUVEC without exposure to 3D-printed materials were included in the experiment as positive controls. Wells filled with medium were included as negative controls. The HUVEC were cultured for 18h with the FDM materials (37°C; 95% air, 5% CO<sub>2</sub>). The viability of the cultures was assessed using an MTT assay, supported by visual inspection of the cell layers.

**Tissue model:** To study the possible effects of the printed materials on incubated tissue, precision-cut liver slices (PCLS; Wistar rats) were chosen as a model. The prepared PCLS have a diameter of 5 mm and a thickness of about 200  $\mu\text{m}^3$ . The use of these dimensions ensures that the slice contains several functional liver units and therefore serves as a good representative for the entire organ. All experiments were approved by the Animal Ethical Committee of the University of Groningen. Preparation of PCLS was done based on the protocol by De Graaf *et al.*<sup>3</sup> Under isoflurane/O<sub>2</sub>

anesthesia, the livers from male Wistar rats (300 g, free access to food and water; Charles River, Sulzfeld, Germany) were excised and placed in ice-cold University of Wisconsin (UW) solution (DuPont Critical Care, Waukegan, IL). Cores (5 mm in diameter) were cut from the livers. A Krumdieck slicer (Alabama R&D, Munford, AL) was used for slicing the cores into precision-cut liver slices which were approximately 200  $\mu\text{m}$  thick, 5 mm in diameter, and had a wet weight of 5 mg. Slices were collected in ice-cold Krebs–Henseleit buffer with 25 mM d-glucose (Merck, Darmstadt, Germany), 25 mM  $\text{NaHCO}_3$  (Merck), and 10 mM HEPES (MP Biomedicals, Aurora, OH) added, and saturated with 95%  $\text{O}_2$  and 5%  $\text{CO}_2$ . PCLS were then transferred to be stored up to 4 hours in ice-cold UW solution until incubation was started.

**Tissue cultivation conditions:** Williams Medium E with L-glutamine (Invitrogen, Paisly, Scotland) (WME), supplemented with 50 mg/mL gentamycin and 25 mM glucose (Invitrogen), was used for incubation. Aliquots of 1.3 mL of WME were added to the wells of a 12-well culture plate. The plates were then equilibrated in a Panasonic (Osaka, Japan) shaking incubator (90 rpm) at 37°C, in which the gas composition was continuously kept at 80%  $\text{O}_2$  and 5%  $\text{CO}_2$ . After the medium had reached 37°C, a slice was inserted in each well, after which the plates were placed in the shaking incubator for 1 hour (pre-incubation). This pre-incubation allowed for the removal of cell debris left over after slicing, and the restoration of PCLS function after the slicing procedure. After pre-incubation, control slices were taken for both the lactate dehydrogenase (LDH) and adenosine triphosphate (ATP) assays. The remaining slices were transferred after pre-incubation to new wells for the 24-h polymer exposure tests, with each slice in its own well together with a 3D-printed ring and fresh, pre-warmed medium. A 24-h slice-incubation period followed at 37°C, 80%  $\text{O}_2$  and 5%  $\text{CO}_2$ . In addition, PCLS without exposure to 3D-printed materials were included in the experiment as positive controls. The viability of the slices was assessed using a fluorescence-based assay for LDH leakage into the medium, and a luminescence-based assay for the ATP content of the slices. For the LDH analysis, a control experiment was performed to assess the possible influence of the 3D-printed polymer rings on the assay itself.

**MTT test (HUVEC):** This assay measures to what extent NAD(P)H-dependent cellular oxidoreductase enzymes reduce the tetrazolium dye 3-(4,5-dimethylthiazol-2-yl)-2,5-diphenyltetrazolium bromide (MTT) to the insoluble compound, formazan. Formazan has a purple color that can be measured by absorbance with a spectrophotometer. The more intense the purple color, the more metabolically active (and viable) the cells.

MTT and sodium dodecyl sulfate (SDS) for the material toxicity study were purchased (Thermo Fisher Scientific Inc.) in the form of the MTT Cell Proliferation Assay Kit. After 18h of incubation, the 3D-printed rings were removed from the wells and EC medium was replaced by EC medium with MTT (10  $\mu\text{L}$  of 12 mM MTT in 100  $\mu\text{L}$  EC medium). The cells were then incubated for 2 hours. After the

reaction, 100  $\mu\text{L}$  of a 0.01 M solution of HCl containing 100 g/L SDS was added to each well and mixed. The well plates were then incubated for 4 hours at 37°C. Afterwards, the absorbance of the samples was measured at 570 nm with a ThermoMax Microplate reader (Molecular Devices, Sunnyvale, CA). Positive controls were included in every experiment. For the positive control HUVEC were cultured in the absence of the 3D-printed material, alongside HUVEC exposed to 3D-printed rings. Negative controls in the experiment were performed in wells without HUVEC and filled only with EC medium, kept under the same conditions and for the same time as HUVEC exposed to 3D-printed rings.

**LDH leakage assay (PCLS):** LDH leakage into the medium was used as an indicator of cell membrane integrity. After 1h of pre-incubation, 3 control slices were each collected in 1.3 mL of fresh WME. After 24 hours, 200- $\mu\text{L}$  samples of medium were taken from all wells. Samples were stored at 4°C for no longer than 24 hours until measurement, to avoid degradation of the LDH. Control slices were homogenized using a bead beater (45 s, Biospec Products, Bartlesville, OK) and centrifuged (16,100 g; 2.5 minutes), after which the supernatant was used for the assay. LDH was measured using the CytoTox-ONE Homogenous Membrane Integrity assay kit (Promega, Madison, WI). Fifty  $\mu\text{L}$  of sample was mixed with an equal amount of the substrate mix at room temperature in a black 96-well plate. After 10 minutes, the reaction was stopped by adding 25  $\mu\text{L}$  of stop solution to each well. Fluorescence intensity was measured at 590 nm after excitation at 560 nm using a Spectramax Gemini XPS fluorescence plate-reader (Molecular Devices, Sunnyvale, CA). LDH baseline was obtained by assessment of the LDH content in PCLS (for every batch separately) not submitted to an experiment, taken after pre-incubation. The LDH leakage of slices for a given experiment was compared to this baseline LDH content. Positive controls were established by unexposed PCLS incubation for the same time and the same conditions as PCLS exposed to 3D-printed materials.

The possible influence of the 3D-printed materials on the fluorescence intensity in this test was also determined. Samples were taken from the medium in which printed rings were incubated without PCLS for 24 hours, and analyzed using the same protocol described above.

**ATP and protein content assay (PCLS):** ATP content was used as an indicator of the ability of the slices to synthesize ATP, the most abundant chemical energy-carrier in the cell. After 24 hours of incubation, slices were collected, transferred to 1 mL of 2 mM EDTA in 70% ethanol (pH 10.9), immediately frozen in liquid nitrogen and stored at -80°C until measurement. For analysis, the slices were thawed on ice and then homogenized using a bead beater (45 s, Biospec Products, Bartlesville, OK) and centrifuged (16,100 g; 5 minutes; 4°C). The supernatant was taken and diluted 10 times with 0.1 M Tris HCl buffer (with 2 mM EDTA; pH 7.8). ATP assessment was done in a black 96-well plate using the Bioluminescence Assay Kit CLS II (Roche, Mannheim, Germany) and an ATP calibration line, measured according to the protocol supplied by the manufacturer. Luminescence was measured

with a LumiCount plate reader (Packard BioScience, Downers Grove, IL). To normalize for the size of the slices, the protein content of the same slices was determined. For this, the slice homogenate was dried and incubated for 30 minutes at 37°C in 200 µL of 5 M NaOH. Eight hundred µL of ultrapure H<sub>2</sub>O was added, after which the samples were homogenized again (45 s) with the bead beater. Protein content was measured with the Bio-Rad DC Protein Assay (Bio-Rad, Munich, Germany), using a calibration line obtained with standard samples of bovine serum albumin. Absorbance was measured at 650 nm with a ThermoMax Microplate Reader (Molecular Devices, Sunnyvale, CA). To account for the varying ATP content of different livers, the normalized ATP content (pmol/µg protein) was expressed as a percentage of the average ATP content of the positive control slices for that experiment. For the positive control, PCLS were incubated in the absence of the 3D-printed material, alongside PCLS exposed to 3D-printed rings. Moreover, during each experiment three slices were taken and frozen right after pre-incubation to confirm viability of the liver used in that experiment.

**Data analysis:** Three different rat livers and three different batches of HUVEC were used for the experiments, using triplicates for each material (n = 3). Outliers were removed based on both statistical analysis (Grubbs test) and visual inspection of the data (boxplots). After these were removed, R software (v. 3.02, Vienna, Austria) was used to perform ANOVA with a post-hoc Tukey's honest significance test to identify significantly different means in all viability assays. A p-value of ≤ 0.05 was considered as indicative of a significant difference. If no significant difference in assay outcome was observed compared to the relevant control experiment, the classification 'biocompatible (+)' was assigned. A significantly different outcome led to a classification of 'not biocompatible (-)'.

### ***Protocol S7: PDMS replication and device fabrication***

Two different negative masters for PDMS replication were 3D printed in red PLA. The slice and print parameters can be found in Table S1. The first master was used to replicate straight channels in PDMS with an aspect ratio of 1 (height = width). Structures were 15 mm long, and the widths and heights were varied between 0.3 and 5.0 mm. The second master contained a single, complex channel (0.15 mm height, 0.3 mm width). The 3D-printed masters were placed in a vacuum desiccator for 20 minutes with a plastic cup, containing a few drops of hexamethyldisilazane (HMDS, Sigma Aldrich, Steinheim, Germany). This would later facilitate the removal of cured PDMS from the masters, probably by the formation of a thin hydrophobic coating over the printed parts. The part was then thoroughly rinsed with water. Elastomer and curing agent for PDMS (Dow Corning, Auburn, MI) were mixed 10:1 (m/m) and stirred for a few minutes. The mixture was placed in a vacuum desiccator for 30 minutes to remove air bubbles from the liquid polymer mixture, then poured onto the master and allowed to cure overnight at 40°C on a hot plate. After curing, the PDMS was peeled from the master. Inlet and outlet holes were punched into the PDMS with a biopsy puncher (d = 1.5 mm, Kai Medical, Solingen, Germany). The channels were sealed by bonding the PDMS replicate to a flat slab of cured PDMS. This was achieved by first exposing both parts to oxygen plasma for 30s (29.6W, 350 mTorr) in a plasma cleaner (PDC-0002, Harrick Plasma, Ithaca, NY), after which the parts were pressed together. Devices were firmly bonded by the time they were employed, in less than 10 minutes in some cases. The channels were filled with a solution of blue dye dissolved in water/methanol (1:1 (v/v)) for visualization.

**Protocol S8:** Wax patterning for paper microfluidics with 3D-printed tools

A 3D-printed tool was used for the wax-dipping method, as published by Songjaroen *et al.*<sup>4</sup> The tool consists of 3 parts, as shown in the Figure S4. The base of the tool with (1) a handle, (2) holes for screws and (3) one smooth surface was 3D printed in PLA (SI, Figure S4A). The smooth surface on the first printed layer was obtained by minimizing the distance between the print bed and the nozzle to below 100  $\mu\text{m}$ , which led to better spreading of deposited polymer on the print bed and thus a smooth surface. A mask for wax patterning was 3D printed in PLA as well (Figure S4B). This mask was designed to shield specific regions from wax deposition, so that they would remain hydrophilic. Chromatography paper was placed between the base and the mask. A third PLA structure was printed and placed on top of the assembly to provide additional pressure on the mask centrally (Figure S4C). The total assembly was screwed together tightly.

Paraffin wax (Sigma Aldrich, Steinheim, Germany) was melted in a beaker on a hotplate set to 120°C. The assembled tool with the paper was dipped in the molten wax for approximately one second, after which the assembly was withdrawn from the wax and the paper subsequently removed from the assembly. Excess wax on the paper was removed with a scalpel. Four masks with different hydrophilic channel widths (0.5, 1.0, 1.5, 2.0 mm) were used to produce paper microfluidic structures ( $n = 5$  per mask), which were then photographed under the microscope with a ruler for size calibration. The channel width was determined with ImageJ<sup>1</sup>.

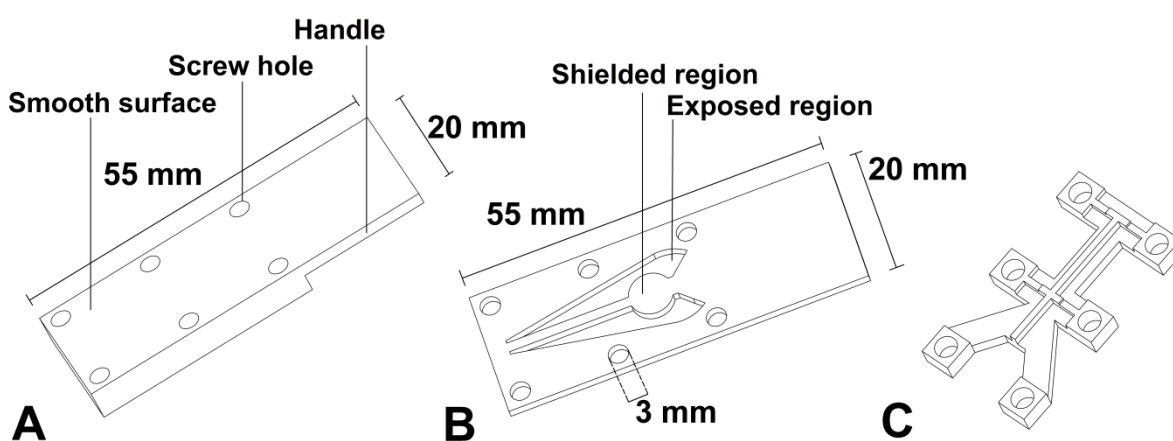


**Figure S4:** SolidWorks drawings for the parts used in the 3D-printed tool made for patterning paper analytical devices with the wax-dipping approach. (A) The flat base with screw holes on to which the paper to be patterned is placed; (B) this drawing shows the 3D-printed mask with openings through which molten wax can contact the paper, making it hydrophobic; (C) structure with screw holes to apply additional pressure on the mask in the center.

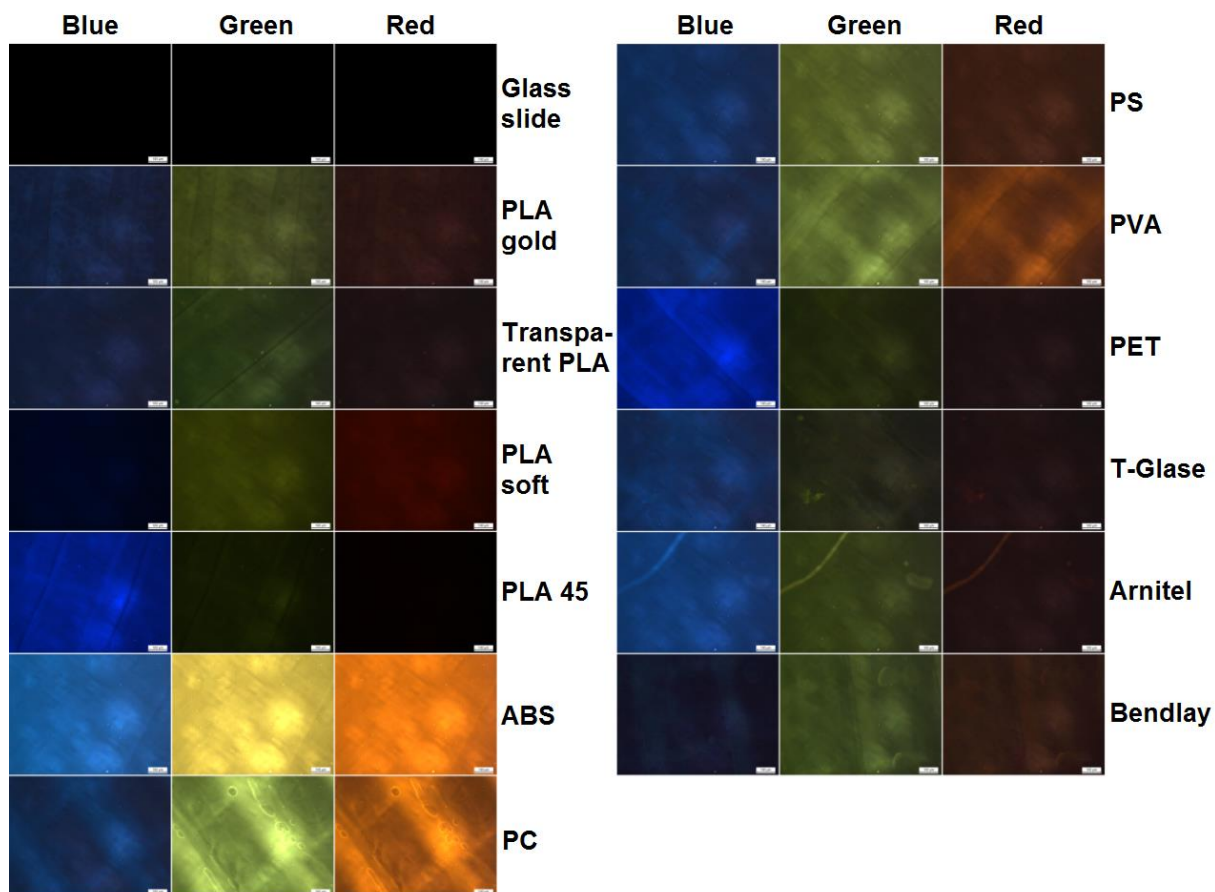


**Figure S5:** Autofluorescence of the twelve FDM materials in the blue (ex/em 430-445/460-500 nm), green (ex/em 450-488/505-545 nm) and red (ex/em 530-557/575-647 nm) range, as compared to glass (black images, top left).



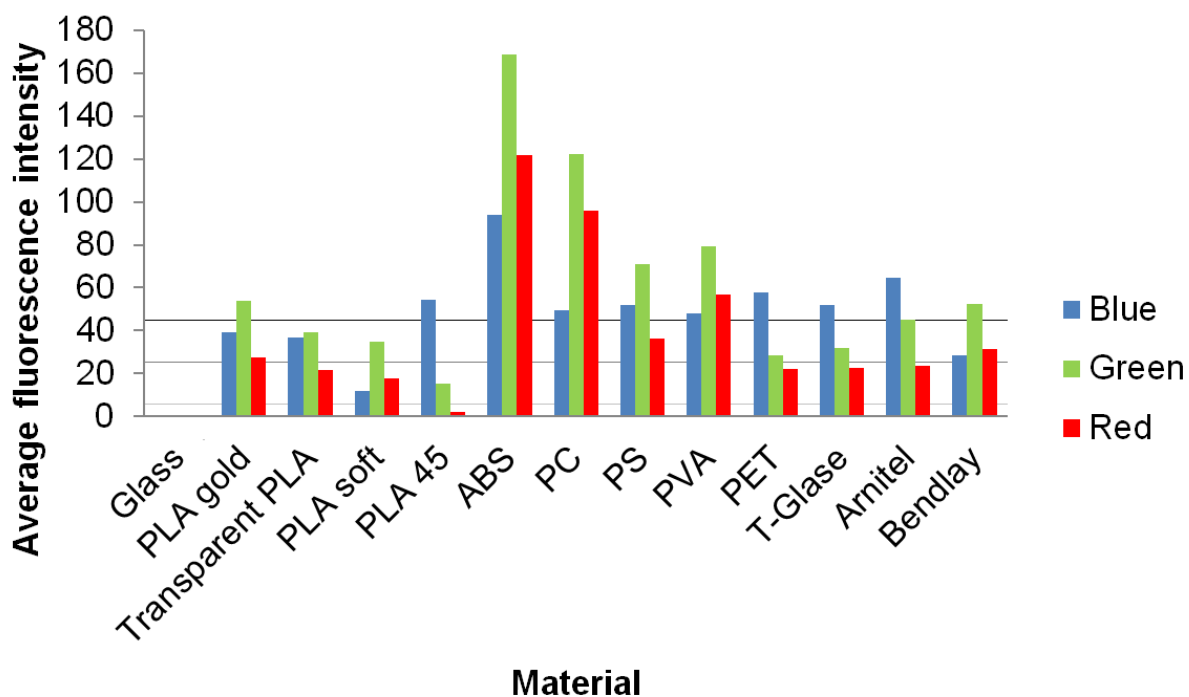


**Figure S6:** Numerical data for the autofluorescence test. The average color intensity (i.e. the average of the intensities for the red, green and blue components of the RGB model) of the photographs in Figure S5 was measured with ImageJ (max. value is 255, which represents a white pixel). Autofluorescence was considered negligible (-) if the value remained below 5, acceptable (+/-) between 5 and 25, strong (+) between 25 and 45 and very strong (++) above 45. These thresholds are indicated by the straight horizontal lines in the graph.

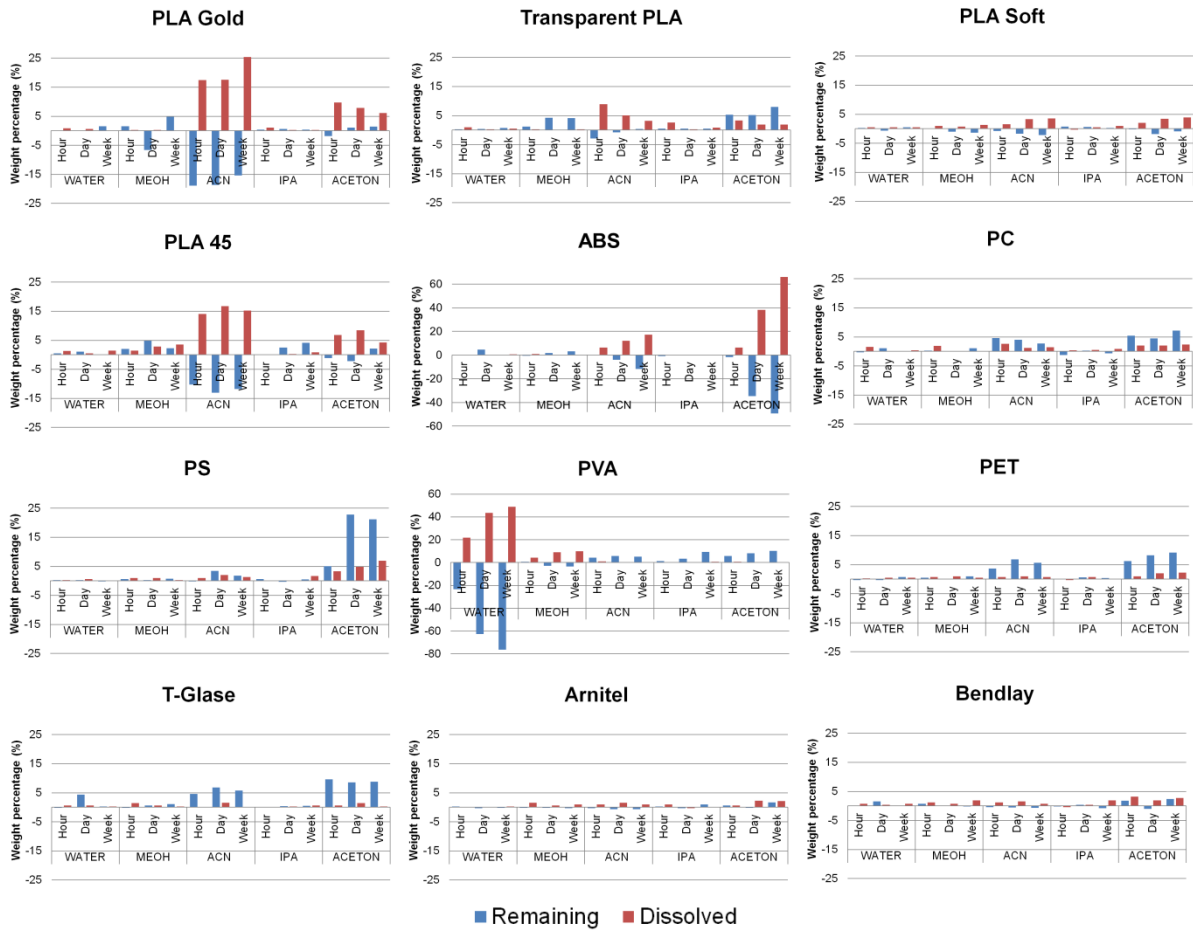


**Figure S7:** Solvent compatibility study for 12 FDM filaments. 3D-printed figures were exposed to five different solvents (water, methanol (MeOH), acetonitrile (ACN), isopropanol (IPA), and acetone) for (i) an hour, (ii) a day (24h), or (iii) a week (168h) as described in Protocol S1. The amount of material which had dissolved into the solvent was determined by weighing the residue in the evaporation tube after complete evaporation (red). Similarly, the change in the amount of material making up the initial structure was determined by weighing the dry structure in the exposure tube (blue). These amounts were all related to the original weight of each figure.

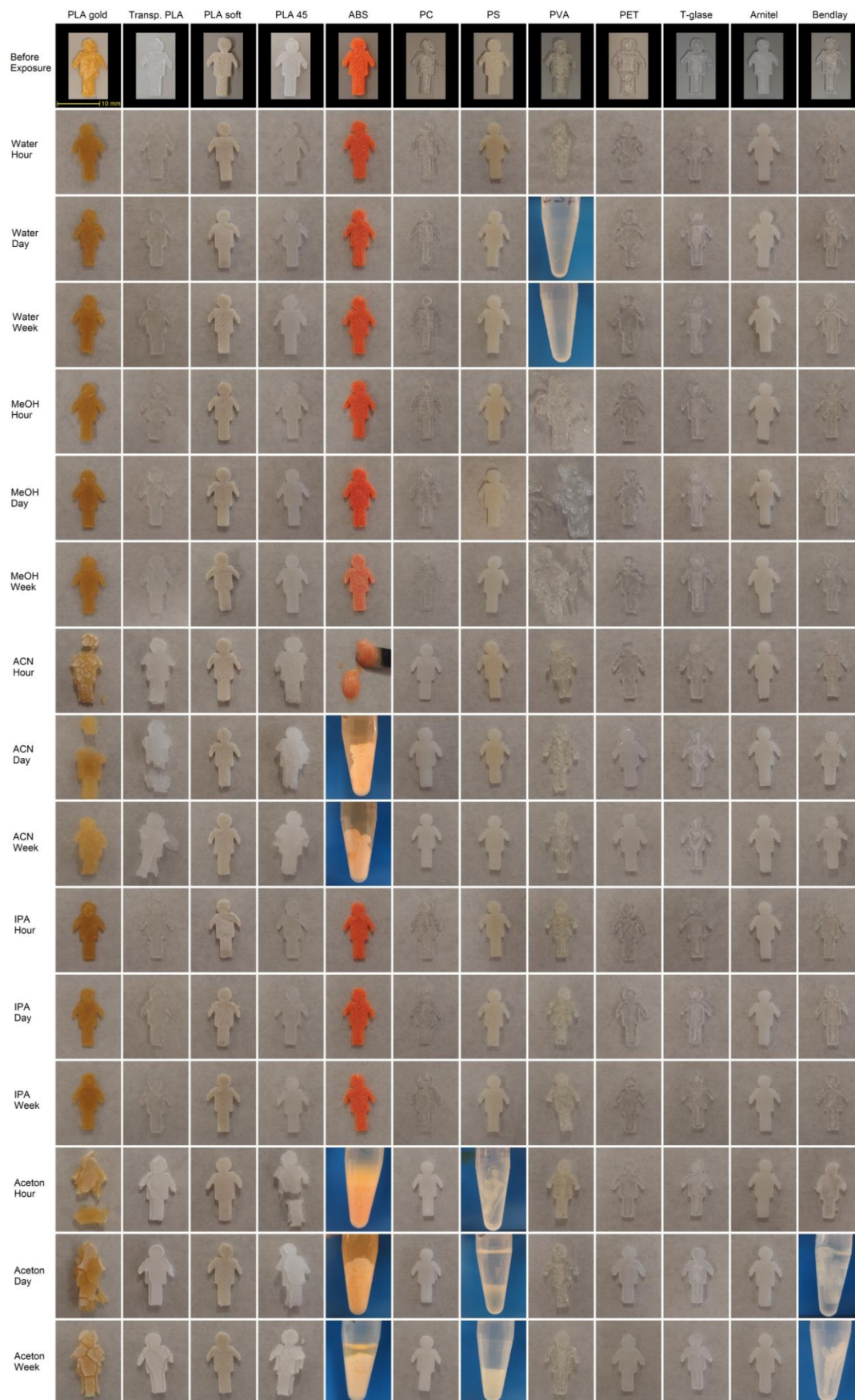


**Figure S8:** Photographs of 3D-printed figures after exposure to different solvents for an hour, a day (24h) or a week (168h). In some cases, loss of integrity of the figures was rapid and/or extreme.

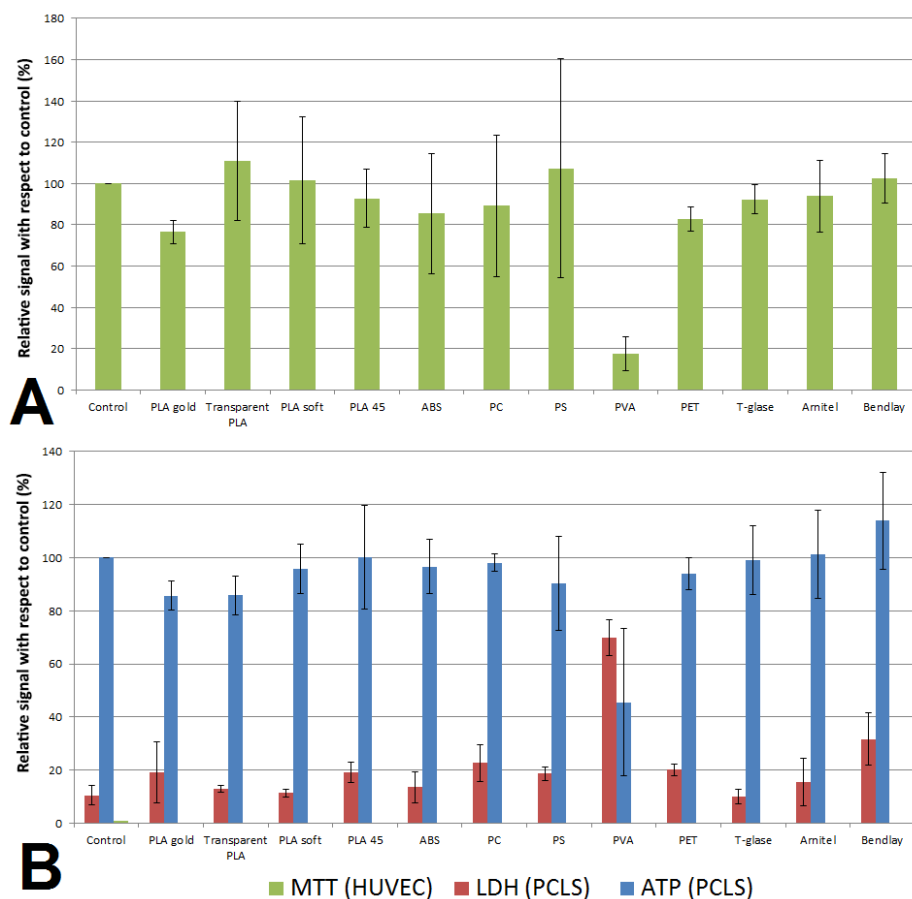


**Figure S9: Biocompatibility of the FDM materials.** (A) Absorbance values for HUVEC incubated for 18h with different 3D-printed materials relative to the positive control. All 3D-printed materials show biocompatibility with HUVEC cultures except PVA ( $p=0.009$ ). This data was collected in three independent experiments (3 cell batches), each performed in triplicate for every material. Large standard deviations are caused by the different numbers of cells in the confluent HUVEC layers. This cell type will modify its size and shape in order to create space for proliferated cells, which resulted in different observed cell densities in the experiments. Furthermore, proliferation rates of HUVEC from the same source might vary because of the cell passage number. In our experiments, we used HUVEC from passage 3 (two experiments) and 4 (one experiment), which is generally accepted in experiments with these cells. They are known to retain their *in vivo* phenotype *in vitro* during early passages. (B) LDH leakage is expressed as a percentage of the average LDH content of control slices measured after the pre-incubation step. Most LDH leakage into the medium occurs during this pre-incubation ( $39\pm 25\%$ ; see Figure S12), as the slices recover from the slicing procedure and cell debris is removed. After 24 hours of incubation in fresh medium with printed polymer rings, slices incubated with all materials show some leakage of LDH into the medium. However, only the amount of LDH leaked out of slices incubated with a PVA ring differs significantly ( $p=2*10^{-7}$ ) from the control group, where PCLS were incubated for 24 hours with no printed material. ATP content, normalized for the protein content, is expressed as a percentage of the average, normalized ATP content of the control slices (24 hours of incubation with no printed material). The control slices are therefore considered as having a 100% normalized ATP content. After 24 hours of incubation none of the groups showed a significant deviation from the control group, except PVA ( $p=0.002$ ).

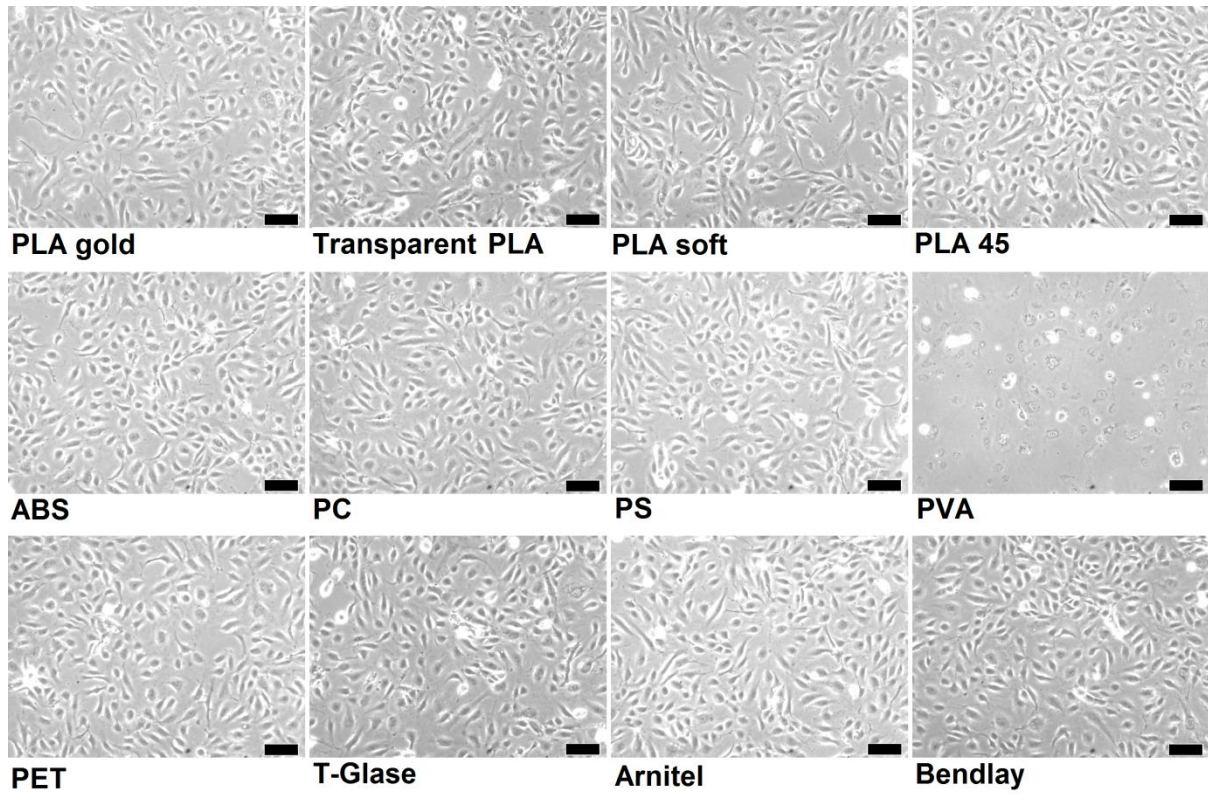


**Figure S10:** Photos of HUVEC cultures acquired after 18h of exposure to 3D-printed materials in 12-well plates. Only PVA shows toxicity towards the HUVEC, as can be concluded by the fact that few HUVEC remain, and those that are still visible are small and misshapen. Magnification of the objective was 10x. The scale bar represents 100  $\mu\text{m}$  (bottom right corner).

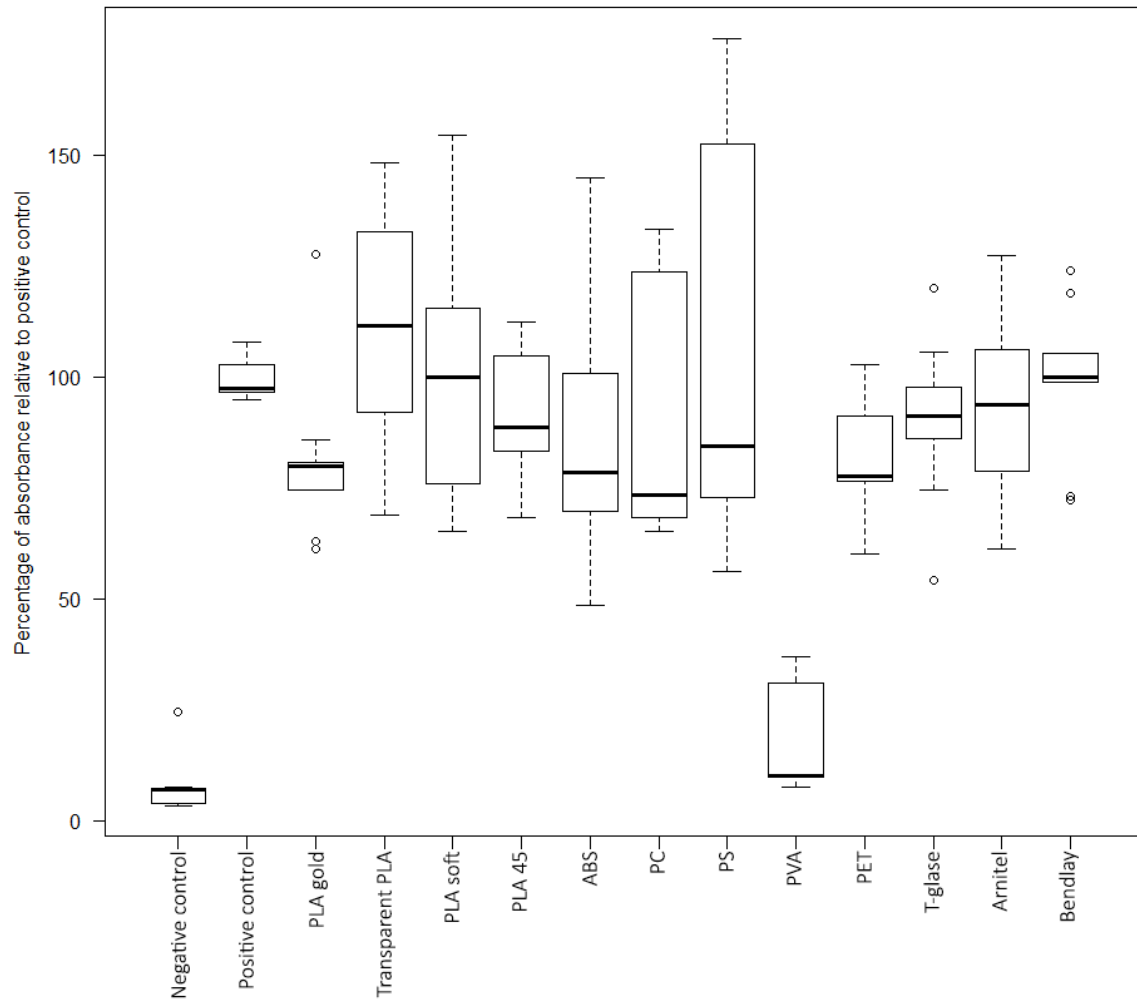


**Figure S11:** Boxplot of the results of the MTT assay on HUVEC cultured with 3D-printed materials. The boxplots were used to visually identify outliers in the data (small circles outside the boxes and whiskers of the plots). These data points were removed prior to calculation of means and standard deviations and performance of ANOVAs.

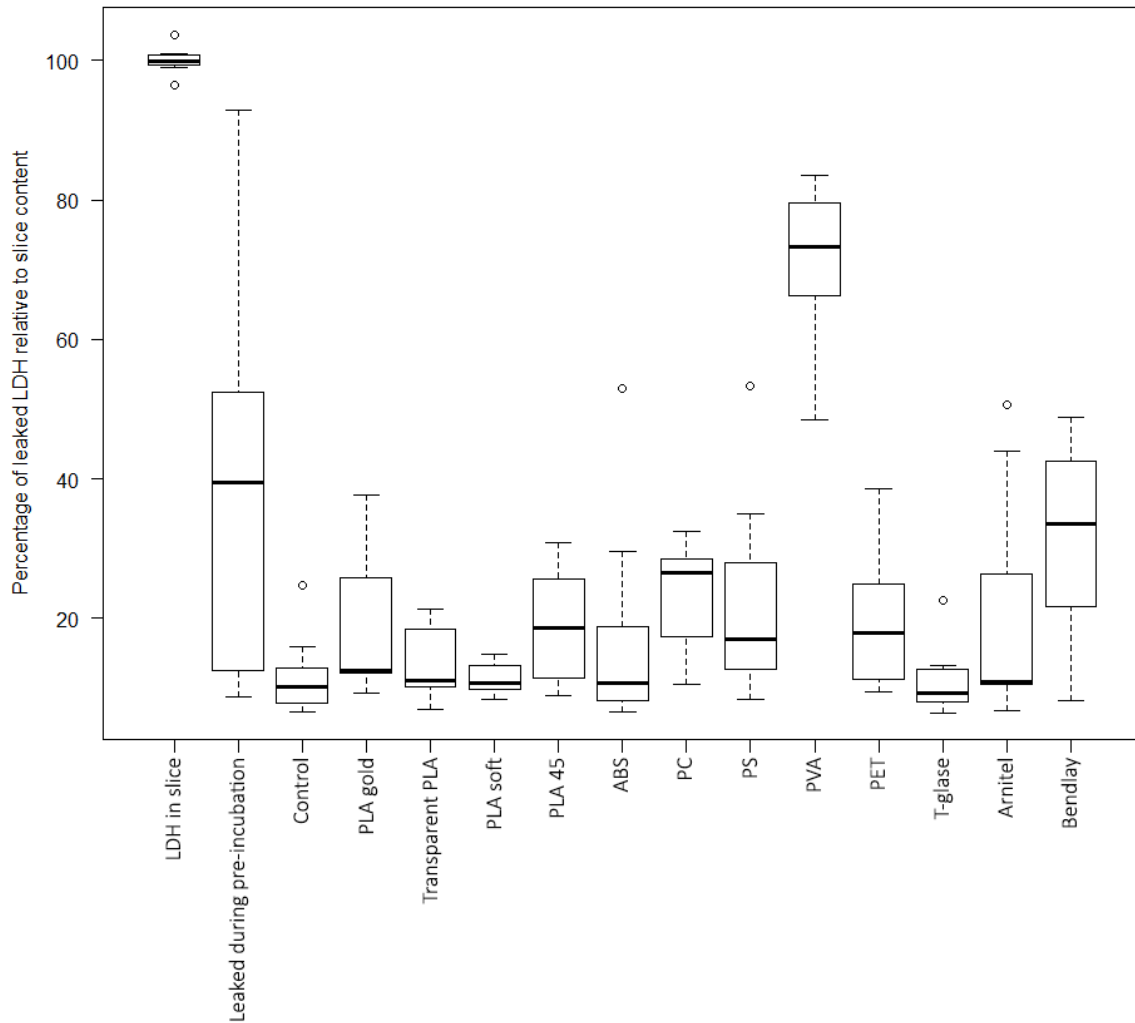


**Figure S12:** Boxplot of the results of the LDH assay on PCLS cultured with various materials. The boxplots were used to visually identify outliers in the data (small circles outside the boxes and whiskers of the plots). These data points were removed prior to calculation of means and standard deviations and performance of ANOVAs. The large variation in LDH content leaked during pre-incubation is as expected<sup>5</sup>, as the pre-incubation serves to remove cellular debris resulting from the slicing procedure<sup>6</sup>.

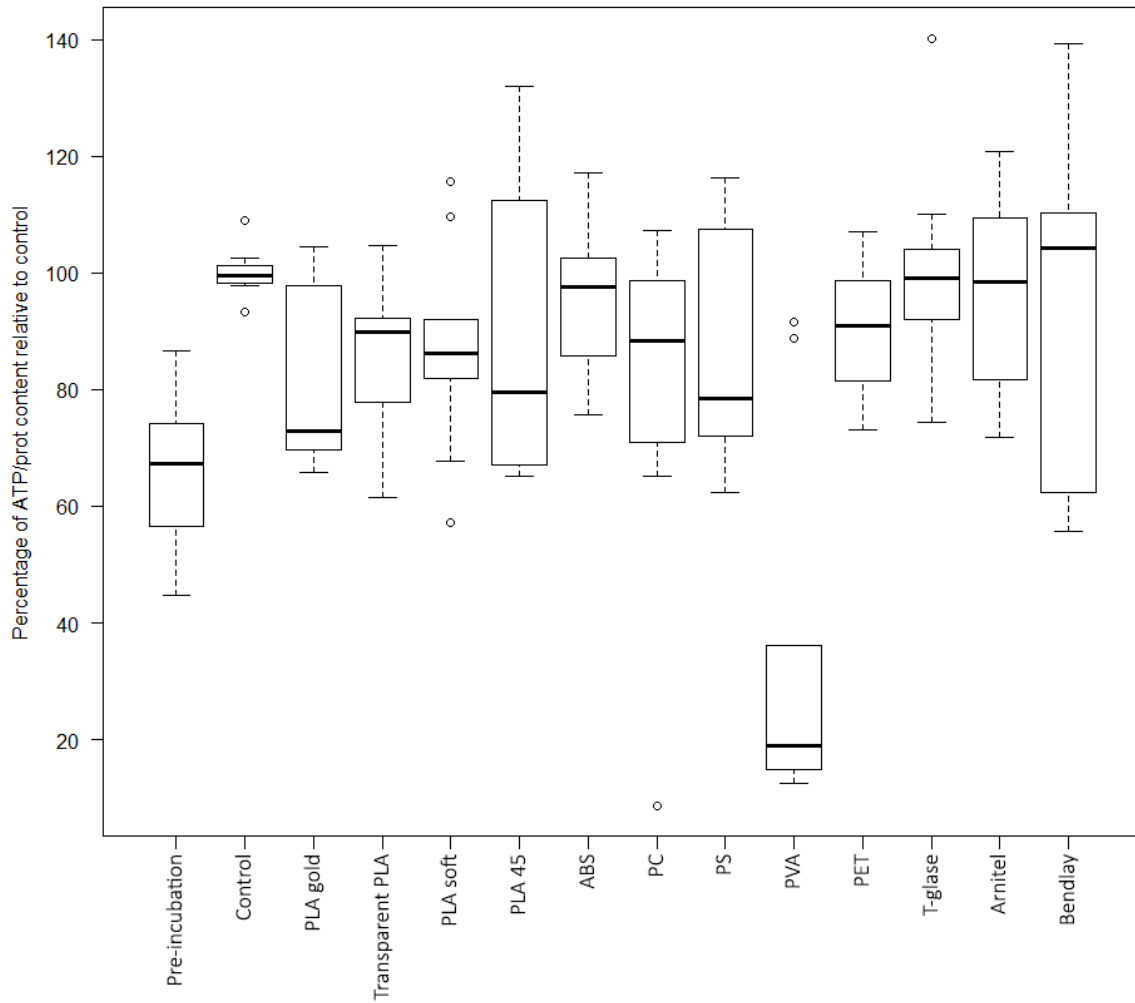


**Figure S13:** Boxplot of the results of the ATP assay on PCLS cultured with various materials (relative to protein content). The boxplots were used to visually identify outliers in the data (small circles outside the boxes and whiskers of the plots). These data points were removed prior to calculation of means and standard deviations and performance of ANOVAs.



## **References**

- 1 C. A. Schneider, W. S. Rasband and K. W. Eliceiri, *Nat. Methods*, 2012, **9**, 671–675.
- 2 T. Bachetti and L. Morbidelli, *Pharmacol. Res.*, 2000, **42**, 9–19.
- 3 I. A. M. de Graaf, P. Olinga, M. H. de Jager, M. T. Merema, R. de Kanter, E. G. van de Kerkhof and G. M. M. Groothuis, *Nat. Protoc.*, 2010, **5**, 1540–1551.
- 4 T. Songjaroen, W. Dungchai, O. Chailapakul and W. Laiwattanapaisal, *Talanta*, 2011, **85**, 2587–2593.
- 5 P. M. Van Midwoud, G. M. M. Groothuis, M. T. Merema and E. Verpoorte, *Biotechnol. Bioeng.*, 2010, **105**, 184–194.
- 6 D. K. Obatomi, S. Brant, V. Anthonypillai, D. A. Early and P. H. Bach, *Toxicol. Vitro.*, 1998, **12**, 725–737.